AN EXPERIMENTAL AND THEORETICAL STUDY OF FREEZING OF PURE ALUMINUM

F. Talati Kalasar and E. Khoshravan

Department of Mechanical Engineering, Faculty of Engineering
University of Tabriz, Tabriz, Iran, ekhosh@ark.tabrizu.ac.ir

(Received: May 9, 2001 – Accepted in Revised Form: April 14, 2002)

Abstract In this work, Boltzmann transform has been used to analyze the problem of freezing of pure Aluminum in semi-infinite domain. The uniqueness of solution (solidification front location) has been proved using the characteristics of the functions appeared in solution. The effect of density change on temperature distribution and errors resulting from ignoring this change have been investigated. The solidification problem in finite media was solved using the boundary element method (BEM), with quadratic shape functions. The applicability of the fundamental solution, as weighting function in BEM, in finite domain has been investigated. The accuracy of the method is illustrated through one-dimensional numerical examples. Some careful experiments were carried out, using the facilities of the School of Metallurgy and Materials at the University of Birmingham, UK, to obtain the data. Comparison of theoretical, numerical and experimental results revealed that good agreement exists between them. However, minor differences were observed due to imposing of the simplifying boundary conditions. The effects of density change may be ignored in small volumes, but they must be taken into account in real applications.

Key Words Phase Change, Moving Boundary, Interface, Gradient, Stefan Problem

چکیده در این مقاله از تبدیل بولتزمان برای تحلیل مسئله انجماد آلومینیم خالص در یک محیط نیمه بیکران استفاده شده و یکتایی جواب مسئله با استفاده از خواص توابع ظاهر شونده در حل مسئله اثبات گردیده است. اثرات تغییر چگالی روی توزیع دما و خطاهای ناشی از اغماض این تغییرات بررسی شده است. مسئله انجماد آلومینیم خالص در محیط محدود با روش اجزاء مرزی و با استفاده از توابع شکل درجه دوم حل گردیده است. معادله رسانش گذرا با استفاده از تابع زمانمند گرین به معادله انتگرال مرزی تبدیل شده و انتگرالهای تلفیقی به طور تحلیلی حل گردیده اند. معادله موازنه انرژی را برای تخمین موقعیت جبهه انجماد بکار برده ایم. مشخصات ماده در دو حالت متفاوت در نظر گرفته شده اند. قابلیت استفاده از جواب اساسی به عنوان تابع وزنی روش اجزاء مرزی بررسی شده است. آزمایشهای فراوانی با استفاده از امکانات فنی دانشکده مواد و متالورژی دانشگاه بیرمنگهام انگلستان برای جمع آوری داده های آنالیز گرمایی انجام دادیم. نتایج شیوه مورد استفاده با نتایج نظری و عددی مقایسه گردیده است. همخوانی جوابها در محدوده قابل قبولی است. از اثرات تغییر چگالی در احجام کوچک می توان صرفنظر کرد، ولی در کاربردهای عملی بایستی این تغییرات را در نظر گرفت.

1. INTRODUCTION

Phase change problems in solidification processing originated about 110 years ago when J. Stefan formulated the problem of finding the temperature distribution and solidification front history of a freezing water slab. Over the last century, particularly in the last 30 years, the problem bearing his name has been extended to include such complex phenomena as the solidification of alloy systems, supercooling.

Analytical or semi-analytical solutions are available only for very simple cases such as one-dimensional semi-infinite geometry with uniform initial temperature and constant imposed boundary temperature and constant thermophysical properties in each phase [1,2]. Such simplified conditions are not of much practical interest. However, these solutions form the backbone of all phase change models and serve as the only means of validating approximate and numerical solutions of complex problems. The literature on general nonlinear heat conduction is vast (a monograph on this problem [3] cites over 900 references). An

exhaustive description of nonlinear boundary value problems can be found in standard monographs [4-7]. Numerical solution of moving boundary problems has been of interest during last three decades. The last those include: Finite Difference Method (FDM), Finite Element Method (FEM) and Boundary Element Method (BEM). A general review of different methods used in simulation of phase change problems can be found in [8-10].

The present paper is concerned with one-dimensional phase transition problems, with particular emphasis on the solidification of castings. The method uses the boundary integral equation to solve the problem.

The governing partial differential equations are reviewed and Boltzmann transform is used to solve the phase change problem in semi-infinte media. The uniqueness of the solution is proved and the effects of density change on temperature distribution are investigated in the first part of the paper. In the second part, the boundary integral equations are solved numerically with quadratic time interpolation functions and the appearing integrals in the formulation are evaluated. Next, experimental procedure to obtain data is described. Finally, numerical and experimental results are presented and discussed.

2. PROBLEM STATEMENT AND ANALYTICAL SOLUTION

We consider a semi-infinite, one-dimensional medium, $0 \le x < \infty$, which is assumed to be occupied originally by a liquid metal of uniform temperature $T_{in} \ge T_m$, where T_m denotes the melting temperature. By imposing a constant temperature $T_o \le T_m$ on the face x=0, solidification starts and progresses to the right. Our goal is to determine the temperature profile and solidification front location. The constancy of density, one of the basic assumptions made in the classical Stefan problem, is not reasonable in many cases. Frozen phase density ρ_f and unfrozen phase ρ_u are assumed to be constants but $\rho_f \neq \rho_u$. Usually, $\rho_f > \rho_u$, so the volume contracts upon solidification. In order to have explicit solution to the problem, it is supposed that the contraction is accompanied by bulk movement of the existing (semi-infinite) phase. The governing equations for the frozen and unfrozen phases are [2]

$$\alpha_f \frac{\partial^2 T_f(x,t)}{\partial x^2} = \frac{\partial T_f(x,t)}{\partial t} \quad 0 < x < X(t), t > 0 \qquad (1)$$

$$\alpha_u \frac{\partial^2 T_u(x,t)}{\partial x^2} = \frac{\partial T_u(x,t)}{\partial t} + V_u(t)\frac{\partial T_u(x,t)}{\partial x} \qquad (2)$$

$$V_u(t) = (1-\frac{\rho_f}{\rho_u})\dot{X}(t) \qquad (3)$$

where α is thermal diffusivity and k is thermal conductivity, and L is the latent heat of fusion. $V_u(t)$ denotes the speed of motion of unfrozen phase, which relates the freezing front velocity to the density ratio. It can be derived using the conservation of the mass between two arbitrary points in the frozen phase and unfrozen phase. The continuity of temperature and the energy balance on the interface must be satisfied. The latter is called Stefan's condition [2]. Using the Boltzmann's transformation [4], (similarity variable $\zeta = \frac{x}{\sqrt{t}}$), one can reduce the above PDEs into ODEs, which are much simpler. Solving the ODEs, we get

$$T_f(x,t) = A_1 \int_0^{\zeta} \exp(-\frac{w^2}{4\alpha_f})dw + A_2 \qquad (4)$$

$$T_u(x,t) = \int_0^{\zeta} A_3 \exp(-\frac{w^2}{4\alpha_u} + \frac{\beta\lambda w(1-\Delta)}{\sqrt{\alpha_u}})dw + A_4 \qquad (5)$$

where $\Delta = \frac{\rho_f}{\rho_u}$, $\beta = \sqrt{\frac{\alpha_f}{\alpha_u}}$, $\lambda = \frac{X(t)}{2\sqrt{\alpha_f t}}$.

The integration constants are found to be

$$A_1 = \frac{T_m - T_o}{\sqrt{\pi\alpha_f}\,\mathrm{erf}(\lambda)},\ A_2 = T_o,$$

$$A_3 = \frac{T_{in} - T_m}{\sqrt{\pi\alpha_u}\,\mathrm{erfc}(\beta\lambda\Delta)}\exp[-(\beta\lambda(1-\Delta))^2]$$

$$A_4 = T_{in} - \frac{T_{in} - T_m}{\text{erfc}(\beta\lambda\Delta)}\text{erfc}[\beta\lambda(\Delta - 1)]$$

Stefan condition leads to a transcendental equation for the parameter λ

$$\frac{St_f}{\lambda e^{\lambda^2}\text{erf}(\lambda)} - \frac{St_u}{\beta\lambda\Delta e^{(\beta\lambda\Delta)^2}\text{erfc}(\beta\lambda\Delta)} = \sqrt{\pi} \quad (6)$$

where $St_f = \frac{C_{pf}(T_m - T_o)}{L}$ and $St_u = \frac{C_{pu}(T_{in} - T_m)}{L}$ denote the Stefan number of frozen phase and unfrozen phase, respectively. It is the ratio of sensible heat to the latent heat. Error function erf ( ) and complementary error function erfc ( ) are defined as follows [11]

$$\text{erf}(x) = \frac{2}{\sqrt{\pi}}\int_0^x e^{-w^2}dw \text{ and } \text{erfc}(x) = 1 - \text{erf}(x)$$

$\text{erf}(x)$ is increasing function while erfc(x) is decreasing one. Furthermore, $\text{erf}(0) = 0$ and $\text{erf}(x) \to 1$ as $x \to \infty$. The Neumann's solution of the Stefan problem is obtained for conditions where the densities are the same, $\Delta = 1$, [2].

The existence theorem guarantees the solution for this problem [11,12] and the uniqueness of the solution may be proved in the following way: Let $f_1(x) = \exp(x^2)\text{erf}(x)$ denote the denominator of the first term in Equation 6

$$\frac{df_1(x)}{dx} = (1 + 2x^2)\exp(x^2)\text{erf}(x) + \frac{2}{\sqrt{\pi}} > 0$$

for all $x > 0$.

$f_1(0) = 0$ and $f_1(x) \to \infty$ as $x \to \infty$.

So, $f_1(x)$ is strictly increasing function, but the function $F_1(x) = \frac{1}{f_1(x)}$ is decreasing one. The denominator of the second term in left-hand side of Equation 6 is the product of two functions; namely, the decreasing function $f_2(x) = \exp(x^2)\text{erfc}(x)$ and increasing function $f_3(x) = xf_2(x)$ for $x > 0$. Their monotonicity properties may be proved as follows:

let

$$g(x) = \exp(-x^2)\frac{df_2(x)}{dx} = 2x\text{erfc}(x) - \frac{2\exp(-x^2)}{\sqrt{\pi}}$$

$$g(0) = \frac{-2}{\sqrt{\pi}} < 0 \text{ and } g(x) \to 0 \text{ as } x \to \infty$$

$$\frac{dg(x)}{dx} = 2\text{erfc}(x) > 0 \text{ for } x > 0$$

It is seen that $g(x) < 0$, whence

$$\frac{df_2(x)}{dx} = g(x)\exp(x^2) < 0 \text{ for } x > 0.$$

Similarly, let

$$h(x) = \exp(-x^2)\frac{df_3(x)}{dx}$$

$$= (1 + 2x^2)\text{erfc}(x) - \frac{2x\exp(-x^2)}{\sqrt{\pi}}$$

$$h(0) = 1 > 0 \text{ and } h(x) \to 0 \text{ as } x \to \infty$$

we conclude that $h(x) > 0$. Thus,

$$\frac{df_3(x)}{dx} = h(x)\exp(x^2) > 0 \text{ for } x > 0.$$

$\Rightarrow f_3(x)$ is increasing function and its inverse $F_2(x) = \frac{1}{f_3(x)}$ is decreasing one.

Denoting the left- hand side of Equation 6 by $f(\lambda)$, it can be written as $f(\lambda) = \lambda\sqrt{\pi}$. The limits of the $f(\lambda)$ are:

$$f(\lambda) \to \infty \text{ as } \lambda \to 0$$
$$f(\lambda) \to -\infty \text{ as } \lambda \to \infty$$

which means that, for $St_f > 0$, $St_u \geq 0$ and $\beta > 0$, the equation $f(\lambda) = \lambda\sqrt{\pi}$ has at least one positive root. i.e. the solution is unique.

Using Maclaurin series for the exponential and error function in Equation 6, one may obtain

$$\lambda_{2-\text{region}} = \frac{1}{2}\left[\frac{St_u}{\beta\lambda\Delta} + \sqrt{2St_f + \left(\frac{St_u}{\beta\lambda\sqrt{\pi}}\right)^2}\right] \quad (7)$$

TABLE 1. Properties of Aluminum Used in Simulation.

$T(^oC)$	$\rho(Kg/m^3)$	$K(W/m^oC)$
20	2699	247
100	2679	245
300	2645	245
500	2599	234
600	2586	232
635	2579	210
660	2561	90
700	2390	110

when $T_{in} = T_m$, or when the specific heat is considerably smaller than the latent heat, ($St_u \approx 0$), we get

$$\lambda_{1-region} = \sqrt{\frac{St_f}{2}} \tag{8}$$

Thus, $\lambda_{1-region} > \lambda_{2-region}$. This of course is expected, since it says that the presence of initial superheating in the unfrozen phase will slow down the solidification process. Because some heat must be removed from the liquid phase to bring unfrozen phase to melting point (T_m) before it can solidify. For materials having extremely small latent heat, ($L \approx 0$), the Equation 6 reduces to

$$\frac{C_{pf}(T_m - T_o)}{e^{\lambda^2}\,erf(\lambda)} = \frac{C_{pu}(T_{in} - T_m)}{\beta\lambda\Delta e^{(\beta\lambda\Delta)^2}\,erfc(\beta\lambda\Delta)} \tag{9}$$

When the initial temperature is equal to melting temperature ($T_{in} = T_m$), we have 1-region Stefan problem, and Neumman's solution is obtained for the classical 1-region Stefan problem [2]. Stefan's condition gives

$$St_f = \lambda\sqrt{\pi}\exp(\lambda^2)erf(\lambda) \tag{10}$$

If the Stefan number is small, one may get

$$T_f(x,t) \approx T_o + (T_m - T_o)\frac{x}{X(t)} \tag{11}$$

which means that the temperature profile at each time is a straight line joining the point ($x=0, T=T_o$) to ($x=X(t), T=T_m$). The Neumann's solution satisfies the diffusion equation and Equation 11 satisfies the steady-state heat equation. It is an approximate solution to 1-phase solidification problem, valid for small Stefan numbers and it is called the quasi-stationary approximation [14]. The quasi-stationary front overestimates the actual front. This overestimation may lead to incorrect results. Equation 6 was solved numerically using Newton-Raphson method, to inspect the dependence of λ on the density ratio Δ, for some values of St_f, St_u, β and for a range of Δ. In practical applications, usually St_f, St_u, β vary between 0.1 and 2, and Δ changes at most by 30%. For these combinations, λ varies linearly with Δ, having small slope, typically $\pm 3.5\%$, (relative to $\Delta=1$ case) when Δ changes by $\pm 30\%$. For most materials, including pure Aluminum, Δ changes by $\pm 10\%$, (Table 1), in most cases one expects 1% variation in λ. Therefore, any quantity proportional to λ is affected very little by the change of density.

The effects of density change may be ignored in small volumes, but they must be taken into account in practical applications. The temperature profile in the unfrozen phase is changed considerably with respect to the $\Delta=1$ case, since it includes the effect of displacement (Equation 5).

The change of density can be related to shrinkage in castings, which leads to the formation of a void at the heat transfer surface. This void may be assumed to act as a thermal resistance layer, having thermal conductivity, k_v, which is much smaller than the thermal conductivity of the frozen phase, k_f. Hence, a reduction in freezing rate results because of the presence of the void [15-16].

3. BOUNDARY INTEGRAL EQUATION AND NUMERICAL IMPLEMENTATION

Several investigators [17-20] have obtained the boundary integral equation corresponding to moving boundary problems. The discretized form of the

these equations may be written as follows

$$\frac{T_o(t_s)-T_m}{2} = -\alpha_f \sum_{j=1}^{S}\int_{t_{j-1}}^{t_j} G_f(0,t_s;0,t_o)q_{oi}\Psi_i dt_o +$$

$$\alpha_f \sum_{j=0}^{S}\int_{t_{j-1}}^{t_j} G_f(0,t_s;X(t_o),t_o)q_{Xi}\Psi_i dt_o \qquad (12)$$

$$0 = \alpha_f \sum_{j=0}^{S}\int_{t_{j-1}}^{t_j} G_f(X(t_s),t_s;X(t_o),t_o)q_{Xi}\Psi_i dt_o$$
$$+\alpha_f \sum_{j=1}^{S}\int_{t_{j-1}}^{t_j} \frac{\partial G_f}{\partial x_o}(X(t_s),t_s;0,t_o)(T_o(t_o)-T_m)\Psi_i dt_o$$
$$-\alpha_f \sum_{j=1}^{S}\int_{t_{j-1}}^{t_j} G_f(X(t_s),t_s;0,t_o)q_{oi}\Psi_i dt_o \qquad (13)$$

where s denotes the number of time steps. The function $G(r_s,t_s;r_o,t_o)$ is the fundamental solution (Green's function) to the heat equation given by [16,20]:

$$G(r_s,t_s;r_o,t_o) = \frac{\exp\{-\frac{(r_s-r_o)^2}{4\alpha(t_s-t_o)}\}}{\sqrt{\{4\pi\alpha(t_s-t_o)\}^n}}$$

where n denotes the number of dimensions of space. $G(r_s,t_s;r_o,t_o)$ represents the temperature at position r_o (observation point or field point) at time t_o due to an instantaneous point source of unit strength located at r_s (source point) releasing its energy spontaneously at time ($t_o = t_s$)[20]. It should be mentioned that although the fundamental solution has been obtained for an infinite domain, it can be used for a finite domain provided that it takes the same values on the boundary of domain as they took in the infinite domain on the fictitious boundary of the actual domain. Thus reproducing on the finite domain the solution of the infinite domain. The unknowns $T_o(t_o)$ and $\frac{\partial T(0,t_o)}{\partial x_o}$ are assumed to vary within each time step according to a quadratic time interpolation function Ψ,

TABLE 2. Values of Interpolation Function at Different Time Stations.

	$t^* = 0$	$t^* = 0.5$	$t^* = 1$
Ψ_1	1	0	0
Ψ_2	0	1	0
Ψ_3	0	0	1

$$\Psi = a(t^*)^2 + bt^* + c \qquad (14a)$$

where $t^* = \frac{t_o - t_{j-1}}{t_j - t_{j-1}}$ is time station. The interpolation function satisfies the conditions, $\Psi_i t_j^* = \delta_{ij}$ where δ_{ij} is the Kronocker delta and $t_1^* = 0$, $t_2^* = \frac{1}{2}$ and $t_3^* = 1$, (Table2).

After computing the coefficients in the above equation, we obtain

$$\Psi_1 = 1 - 3t^* + 2t^{*2},\ \Psi_2 = 4t^* - 4t^{*2},\ \Psi_3 = 2t^{*2} - t^*$$
$$q_o(t) = q_{oi}\Psi_i\ ,\ T_o(t) = T_{oi}\Psi_i \qquad (14b)$$

where q_{oi} and T_{oi} (i=1,2,3) are the values of heat flux and temperature at time stations $t_o = t_{j-1}$, $t_o = t_{j-1/2}$ and $t_o = t_j$, respectively.

The diagram of these interpolation functions is depicted in Figure 1. The integrals appearing in the boundary integral equations are of the following type:

$$I_{1i} = \alpha\int_{t_{j-1}}^{t_j} G(0,t_s;0,t_o)\Psi_i dt_o$$

$$I_{2i} = \alpha\int_{t_{j-1}}^{t_j} \frac{\partial G(0,t_s;0,t_o)}{\partial x_o}\Psi_i dt_o$$

$$I_{3i} = \alpha\int_{t_{j-1}}^{t_j} G(X(t_s),t_s;0,t_o)\Psi_i dt_o$$

$$I_{4i} = \alpha\int_{t_{j-1}}^{t_j} \frac{\partial G(X(t_s),t_s;0,t_o)}{\partial x_o}\Psi_i dt_o$$

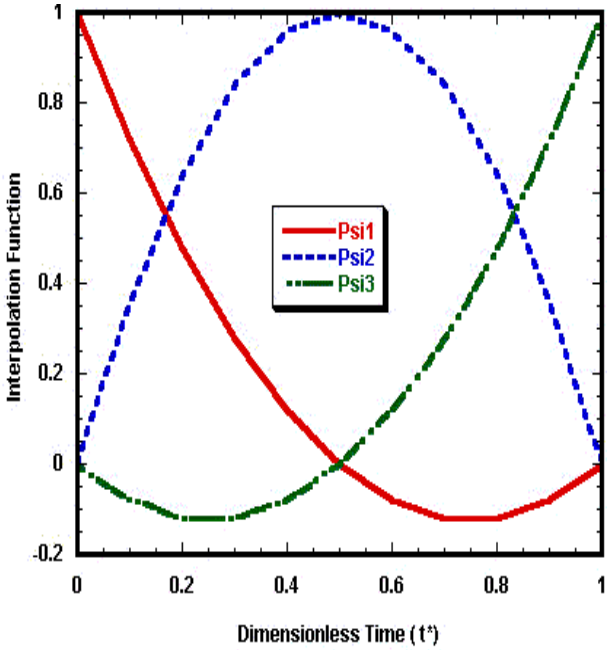

Figure 1. Quadratic time interpolation function used in simulation.

$$I_{5i} = \alpha \int_{t_{j-1}}^{t_j} G(X(t_s), t_s; X(t_o), t_o) \Psi_i dt_o$$

$$I_{6i} = \alpha \int_{t_{j-1}}^{t_j} \frac{\partial G(X(t_s), t_s; X(t_o), t_o)}{\partial x_o} \Psi_i dt_o \qquad (14c)$$

Analytical expressions for the integrals within each time step for interpolation functions $\Psi = \sqrt{t_o}$ and $\Psi = t_o$ have been given in [21,22]. Using shape functions in Equation 14b, one can analytically calculate the integrals appeared in Equation 14c, (see the appendix).

Choosing different locations for source point $X(t_s)$ and field point $X(t_o)$, the following integrals can be written for the coefficients of t and q in each time step $\Delta t_j = t_j - t_{j-1}$

$$H_j^i = \alpha \int_{t_{j-1}}^{t_j} \frac{\partial G(X(t_s), t_s; X(t_o), t_o)}{\partial x_o} \Psi_i dt_o$$

$$M_j^i = \alpha \int_{t_{j-1}}^{t_j} G(X(t_s), t_s; X(t_o), t_o) \Psi_i dt_o$$

The application of the above equations to all boundary nodes gives

$$A^1 T_{j-1} + A^2 T_{j-1/2} + A^3 T_j = B^1 Q_{j-1} + B^2 Q_{j-1/2} + B^3 Q_j \qquad (15)$$

where A^1 is equal to H_j^1 term of time step Δt_j plus H_{j-1}^3 term of time step Δt_{j-1}, A^3 is equal to H_j^3 term of time step Δt_j and H_{j+1}^1 term of time step Δt_{j+1}. The same approach is used for the coefficients B^1 and B^3 (The influence of the common nodes must be taken into account).

After imposing boundary conditions, the resulting equations are arranged such that all the unknowns (that is, heat flux and the velocity of the solidification front) are on the left-hand side of the new matrix equation and the knowns are expressed on the right-hand side.

$$\{K\}[u] = \{f\} \qquad (16)$$

The above set of equations is solved at each time step. The location of freezing front is unknown. Quasi-stationary approximation was used to find the location of freezing front in primary stages of BEM solution. So, all the unknowns are determined up to the time t_{j-1} and it is desired to find the solution at time t_j. Starting with a guess for the velocity of freezing front at time $t = t_j$, we may calculate the position of the moving boundary from following equation

$$X(t_o) = X(t_{j-1}) + V(\overline{t_j})(t_0 - t_{j-1}) \qquad (17)$$

in which $\overline{t_j} = 0.5(t_{j-1} + t_j)$ and solve the system of integral equations. If the estimated position of solidification front were correct, the computed values of velocity and temperature gradient would satisfy the Stefan condition. However, this may not be the case. So, the velocity is to be adjusted using the following expression:

$$\frac{dX(t_j)}{dt} = \frac{1}{2}\left[\frac{dX(t_{j-1})}{dt} + \left(\frac{k}{\rho L}\frac{dT}{dx}\right)_{t_j}\right] \qquad (18)$$

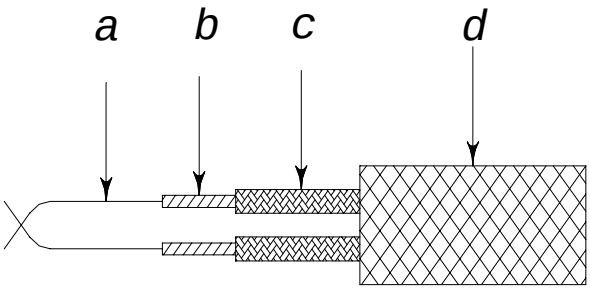

Figure 2. Schematic diagram of construction of thermocouple.

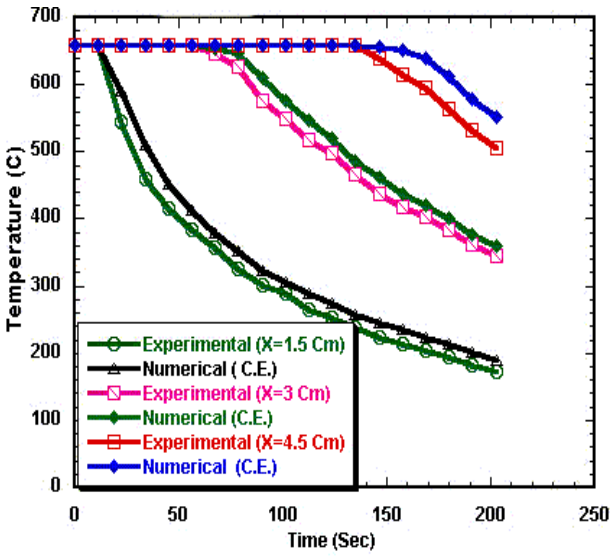

Figure 3. Temperature vs. time (constant shape function).

and the new position of $X(t)$ can be determined. The iteration may be continued until a prescribed condition is satisfied, that is,

$$\left\| \frac{V_{corr} - V_{pr}}{V_{corr}} \right\| \leq \varepsilon \qquad (19)$$

where $V_{corr} = \frac{dX(t_j)}{dt}$, $V_{pr} = \frac{dX(t_{j-1})}{dt}$ and ε denote the corrected velocity, predicted velocity of solidification front and specified tolerance, respectively.

4. EXPERIMENTAL WORK

Experiments were carried out, using the facilities of the School of Metallurgy and Materials of the University of Birmingham, UK. to obtain results which would be compared with the solutions of BEM. The overall geometry of the casting, was a circular bar with a diameter of 25 mm and 100-mm length. The casting was located horizontally to minimize convection currents. The surface and the back face of the pipe were insulated with fiberfrax blanket insulating material and front face was exposed to ambient temperature to create unidirectional solidification. The mould was made from AFS 60 grade washed and dried silica sand, bonded with 1.2 mass % Phenolic Urethane resin (Ashland Pepset). This is a widely used moulding material and it was therefore to be hoped that good material properties would be available. Aluminum with purity of 99.9% was used as liquid metal. This metal has high thermal conductivity, high latent heat of fusion and single-point transition temperature. Rolls Royce kindly provided materials data for mould and casting. Materials data used in the simulation are shown in Table 2. The density of sand was 1520 (kg/m^3).

The charge metal 1.5-kg was poured at approximately 670^oC into pouring basin. The filling time was close to 2.5 seconds. The ambient temperature was 20^oC. The mould was heated up to 670^oC in an electric furnace to create boundary condition used in simulation.

Thermal analysis was carried out using K-type thermocouples, a nickel-chromium/nickel aluminium conductor combination. The thermocouples (Figure 1) consisted of a pair of solid wires (a), which were each double glass fibre lapped (b) and then glass fibre braided and silicone varnished (c). The pair was then laid flat and glass fibre braided overall and impregnated with silicone varnish (d).

Thermocouples were located along the centerline of the casting at different distances from one another. The diameter of thermocouple wire was 0.3 mm and crossing the wire and spot welding created the junction. The excess wire was trimmed off. The wire (with the exception of approximately 1 mm distance from the junction tip) was insulated with white paint (TiO2- containing emulsion paint and subsequently fired to burn off volatiles) to

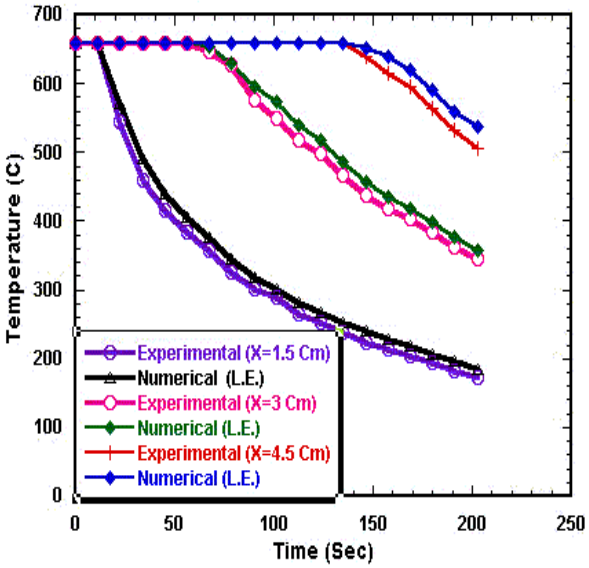

Figure 4. Temperature vs. time (linear shape function).

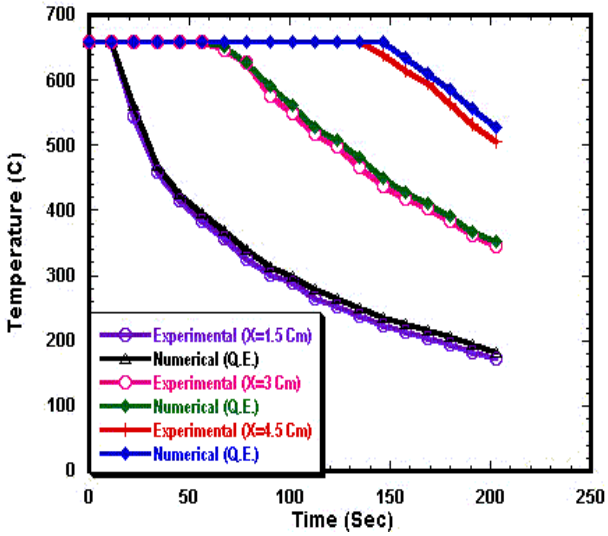

Figure 5. Temperature vs. time (Quadratic shape function).

prevent the possibility of a short circuit by the liquid metal. An effective internal calibration of the thermocouples was performed taking advantage of the fact that pure Aluminum was being frozen, thus defining a temperature close to $659.0^{o}C$, Thus thermocouple readings were adjusted to read about $659.0^{o}C$, during the early part of the plateau region of the cooling curve. Data were logged into a computer at rates selected from 10, 20, 50, 100, 200 and 250 signals per second for different experiments. Different boundary conditions were created during the experiment. In one experiment the front face was maintained at constant temperature by the application of a jet of compressed air to the back mould. In another experiment ensuring that the back of the mould was in relatively still air used convection boundary condition.

5. RESULTS AND DISCUSSION

The example considered is a cylindrical pipe with 25 mm in diameter and 100 mm in length, which is initially filled with liquid metal (Aluminum with purity of 99.9%) at the freezing temperature ($T_{in} = T_m = 659^{o}C$). The surface is cooled suddenly to the ambient temperature T_o. Solidification starts and inwards, the measured and calculated cooling curves at different position of thermocouples are presented in Figures 2-4, for the cases of constant, linear and quadratic elements used in interpolation functions, respectively.

In the first stages of calculations, the time step was chosen $\Delta t = 0.001$ seconds, but it was changed to 0.02 seconds and then to 0.05 seconds at later time steps. Results show that, there exists less restriction on time step size. The number of elements used in simulation was variable between 40 and 100 elements. The CPU time for calculating the values of temperature has been reduced by 16% and 22.5% in the case of linear and quadratic elements in comparison with CPU time of constant elements, respectively.

The calculated values of temperature using the BEM and the measured values differ by 3 to 7 percent in linear elements and quadratic elements, respectively. This is due to the use of quasi-stationary method in the first stage of calculations, which assumes that during a time step, the movement of solidification front is small relative to heat conduction. The difference becomes less and less in later time steps.

The change of density, yields voids formation near the heat transfer surface, between cast and mould, which reduces the rate of heat transfer considerably. The cooling time may increases up to

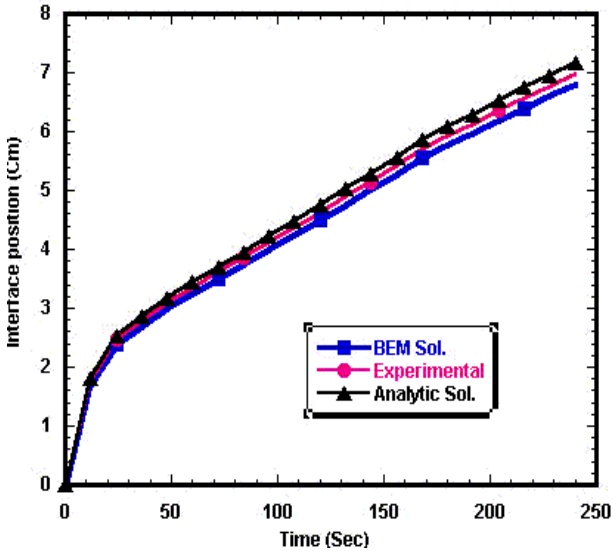

Figure 6. Interface location vs. time.

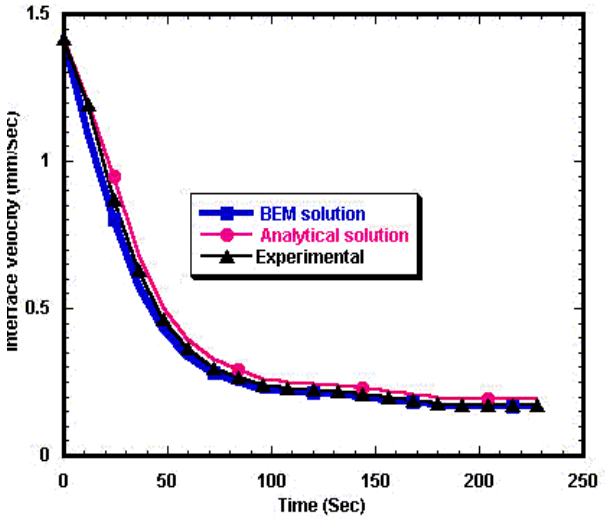

Figure 7. Velocity of freezing front vs. time.

57% of that in case of neglecting this change. The BEM results, for location of interface, are compared with the analytical solution for semi-infinite medium [2] and experimental ones, Figure 6. The agreement between thermal analysis and calculated values from the solution of boundary integral equation appears to be reasonable although some differences may be noted. These differences may be associated to inaccuracies in materials data, heat transfer parameters, poor calibration of thermocouples and different sensitive of thermocouples.

Cooling curves and derivative first curves can be used to identify the end of solidification process. The distance between thermocouples is known, one may read the elapsed time from time axis, to calculate the velocity of freezing front. A rapid drop in temperature was recorded at points very near to the mould surface (implying that rate of solidification is initially high and becomes smaller at large times). As distance from the mould surface increases, temperature gradient decrease, as shown in Figure 7.

6. CONCLUSION

BEM seems to be a useful general method for the analysis of moving boundary value problems. Mesh adjustment in this method is easier than other numerical methods. There is less restriction on time step size compared to other methods. Good agreement for temperature fields during solidification of pure commercial Aluminum is achieved.

7. APPENDIX

$$I_{11}=\sqrt{\frac{\alpha}{\pi}}\{(\sqrt{t_s-t_j}-\sqrt{t_s-t_{j-1}})(\frac{3(t_s-t_{j-1})}{\Delta t_j}+$$

$$\frac{4t_s t_{j-1}-2t_s^2-t_{j-1}^2}{(\Delta t_j)^2}-1)-\frac{1}{5(\Delta t_j)^2}[\sqrt[5]{t_s-t_j}-\sqrt[5]{t_s-t_{j-1}}]\}$$

$$-\frac{1}{3}\sqrt{\frac{\alpha}{\pi}}[\sqrt[3]{t_s-t_j}-\sqrt[3]{t_s-t_{j-1}}](\frac{3}{\Delta t_j}-\frac{4(t_s-t_{j-1})}{(\Delta t_j)^2})$$

$$I_{12}=4\sqrt{\frac{\alpha}{\pi}}\{($$

$$\sqrt{t_s-t_j}-\sqrt{t_s-t_{j-1}})(\frac{t_s^2-t_{j-1}^2-2t_s t_{j-1}}{(\Delta t_j)^2}-\frac{t_s-t_{j-1}}{\Delta t_j})$$

$$+\frac{\sqrt[5]{t_s-t_g}-\sqrt[5]{t_s-t_{j-1}}}{5(\Delta t_j)^2}\}$$

$$+4\sqrt{\frac{\alpha}{\pi}}\{(\sqrt[3]{t_s-t_j}-\sqrt[3]{t_s-t_{j-1}})(\frac{4\Delta t_j-2(t_s-t_{j-1})}{3(\Delta t_j)^2})\}$$

$$I_{13}=\sqrt{\frac{\alpha}{\pi}}\{(\sqrt{t_s-t_j}-\sqrt{t_s-t_{j-1}})(\frac{t_s-t_{j-1}}{\Delta t_j}-$$

$$\frac{2t_s^2+t_{j-1}^2-4t_st_{j-1}}{(\Delta t_j)^2})-\frac{2}{5(\Delta t_j)^2}(\sqrt[5]{t_s-t_j}-\sqrt[5]{t_s-t_{j-1}})\}$$

$$+\sqrt{\frac{\alpha}{\pi}}(\sqrt[3]{t_s-t_j}-\sqrt[3]{t_s-t_{j-1}})(\frac{4(t_s-t_{j-1})-\Delta t_j}{3(\Delta t_j)^2})\}$$

$$I_{2i}=0 \qquad i=1,2,3$$

$$I_{31}=\{(\frac{t_sX}{2}+\frac{X^3}{12\alpha})(\frac{3}{\Delta t_j}+\frac{4t_{j-1}}{(\Delta t_j)^2})$$

$$-\frac{X}{2}(1+\frac{3t_{j-1}}{\Delta t_j}+\frac{2t_{j-1}^2}{(\Delta t_j)^2})-\frac{1}{(\Delta t_j)^2}(t_s^2X+\frac{t_sX^3}{3\alpha}+\frac{X^5}{60\alpha^2}\}$$

$$\times\{\frac{2}{\sqrt{\pi}}\sum_{n=0}^{\infty}\frac{(-1)^n}{(2n+1)n!}[(u_j)^{n+\frac{1}{2}}-(u_{j-1})^{n+\frac{1}{2}}]\}$$

$$+\{(\frac{t_sX}{2\sqrt{\pi}}+\frac{X^3}{12\alpha\sqrt{\pi}})(\frac{3}{\Delta t_j}+\frac{4t_{j-1}}{(\Delta t_j)^2})$$

$$-\frac{X}{2\sqrt{\pi}}(1+\frac{3t_{j-1}}{\Delta t_j}+\frac{2t_{j-1}^2}{(\Delta t_j)^2})$$

$$-\frac{1}{\sqrt{\pi}(\Delta t_j)^2}(t_s^2X+\frac{t_sX^3}{3\alpha}+\frac{X^3}{60\alpha^2})\}$$

$$\times\{\sum_{n=0}^{\infty}\frac{(-1)^n}{n!}[(u_j)^{n-\frac{1}{2}}-(u_{j-1})^{n-\frac{1}{2}}]\}$$

$$-\frac{X^5}{60\alpha^2\sqrt{\pi}(\Delta t_j)^2}\sum_{n=0}^{\infty}\frac{(-1)^n}{n!}[(u_j)^{n-\frac{5}{2}}-(u_{j-1})^{n-\frac{5}{2}}]$$

$$+\{\frac{1}{\sqrt{\pi}(\Delta t_j)^2}(\frac{t_sX^3}{6\alpha}+\frac{X^5}{120\alpha^2})$$

$$-\frac{X^3}{24\alpha\sqrt{\pi}}(\frac{3}{\Delta t_j}+\frac{4t_{j-1}}{(\Delta t_j)^2})\}\times\{\sum_{n=0}^{\infty}\frac{(-1)^n}{n!}[(u_j)^{n-\frac{3}{2}}-(u_{j-1})^{n-\frac{3}{2}}]\}$$

where $u_j=\frac{X^2}{4\alpha(t_s-t_j)}$, $u_{j-1}=\frac{X^2}{4\alpha(t_s-t_{j-1})}$

and $X=X(t_s)$

$$I_{32}=\{2X-(\frac{1}{\Delta t_j}+\frac{2t_{j-1}}{(\Delta t_j)^2})(2t_sX+\frac{X^3}{3\alpha})$$

$$+\frac{2}{(\Delta t_j)^2}(t_s^2X+\frac{t_sX^3}{3\alpha}+\frac{X^5}{60\alpha^2})\}$$

$$\{\frac{2}{\sqrt{\pi}}\sum_{n=0}^{\infty}\frac{(-1)^n}{(2n+1)n!}[(u_j)^{n+\frac{1}{2}}-(u_{j-1})^{n+\frac{1}{2}}]$$

$$+\frac{X^5}{30\sqrt{\pi}\alpha^2(\Delta t_j)^2}\{\sum_{n=0}^{\infty}\frac{(-1)^n}{n!}[(u_j)^{n-\frac{5}{2}}-(u_{j-1})^{n-\frac{5}{2}}]\}$$

$$+\{\frac{2}{(\Delta t_j)^2\sqrt{\pi}}(t_s^2X+\frac{t_sX^3}{3\alpha}+\frac{X^5}{60\alpha^2})$$

$$(\frac{2X}{\sqrt{\pi}}-(\frac{1}{\Delta t_j}+\frac{2t_{j-1}}{(\Delta t_j)^2})(\frac{2t_sX}{\sqrt{\pi}}+\frac{X^3}{3\alpha\sqrt{\pi}})$$

$$\times\{\sum_{n=0}^{\infty}\frac{(-1)^n}{n!}[(u_j)^{n-\frac{1}{2}}-(u_{j-1})^{n-\frac{1}{2}}]\}$$

where $u_j=\frac{X^2}{4\alpha(t_s-t_j)}$, $u_{j-1}=\frac{X^2}{4\alpha(t_s-t_{j-1})}$

and $X=X(t_s)$

$$I_{33}=\{(\frac{4t_{j-1}}{(\Delta t_j)^2}+\frac{1}{\Delta t_j})(\frac{t_sX}{2}+\frac{X^3}{12\alpha})$$

$$-\frac{X}{2}(\frac{2t_{j-1}^2}{(\Delta t_j)^2}+\frac{t_{j-1}}{\Delta t_j})$$

$$-\frac{1}{(\Delta t_j)^2}(t_s^2X+\frac{t_sX^3}{3\alpha}+\frac{X^5}{60\alpha^2})\}$$

$$\times\{\frac{2}{\sqrt{\pi}}\sum_{n=0}^{\infty}\frac{(-1)^n}{(2n+1)n!}[(u_j)^{n+\frac{1}{2}}-(u_{j-1})^{n+\frac{1}{2}}]\}$$

$$-\{(\frac{4t_{j-1}}{(\Delta t_j)^2}+\frac{1}{\Delta t_j})(\frac{t_sX}{2\sqrt{\pi}}+\frac{X^3}{12\alpha\sqrt{\pi}})$$

$$-\frac{X}{2\sqrt{\pi}}(\frac{2t_{j-1}^2}{(\Delta t_j)^2}+\frac{t_{j-1}}{\Delta t_j})$$

$$-\frac{1}{\sqrt{\pi}(\Delta t_j)^2}(t_s^2X+\frac{t_sX^3}{3\alpha}+\frac{X^5}{60\alpha^2})\}$$

$$\times\{\sum_{n=0}^{\infty}\frac{(-1)^n}{n!}[(u_j)^{n-\frac{1}{2}}-(u_{j-1})^{n-\frac{1}{2}}]\}$$

where $u_j = \frac{X^2}{4\alpha(t_s - t_j)}$, $u_{j-1} = \frac{X^2}{4\alpha(t_s - t_{j-1})}$

and $X = X(t_s)$

$$I_{41} = \{\frac{1}{2}(1 + \frac{t_{j-1}}{\Delta t_j} + \frac{2t_{j-1}^2}{(\Delta t_j)^2}) -$$

$$(\frac{3}{\Delta t_j} + \frac{4t_{j-1}}{(\Delta t_j)^2})(\frac{t_s}{2} - \frac{X^2}{4\alpha}) + \frac{t_s^2}{(\Delta t_j)^2} - \frac{X^4}{12\alpha^2(\Delta t_j)^2} - \frac{t_s X^2}{\alpha(\Delta t_j)^2}\}$$

$$\times\{\frac{2}{\sqrt{\pi}}\sum_{n=0}^{\infty}\frac{(-1)^n}{(2n+1)n!}[(u_j)^{n+\frac{1}{2}} - (u_{j-1})^{n+\frac{1}{2}}]\}$$

$$-\{\frac{t_s^2 X^4}{2(\Delta t_j)^2\alpha^3\sqrt{\pi}} + \frac{X^4}{12\sqrt{\pi}\alpha^2(\Delta t_j)^2} +$$

$$\frac{X^2}{4\alpha\sqrt{\pi}}(\frac{3}{\Delta t_j} + \frac{4t_{j-1}}{(\Delta t_j)^2})\}$$

$$\times\{\sum_{n=0}^{\infty}\frac{(-1)^n}{n!}[(u_j)^{n-\frac{1}{2}} - (u_{j-1})^{n-\frac{1}{2}}]\}$$

$$-\frac{(X(t_s))^4}{24\alpha^2\sqrt{\pi}(\Delta t_j)^2}(\sum_{n=0}^{\infty}\frac{(-1)^n}{n!}[(u_j)^{n-\frac{3}{2}} - (u_{j-1})^{n-\frac{3}{2}}]$$

where $u_j = \frac{X^2}{4\alpha(t_s - t_j)}$, $u_{j-1} = \frac{X^2}{4\alpha(t_s - t_{j-1})}$

and $X = X(t_s)$

$$I_{42} = \{\frac{2}{\sqrt{\pi}}\sum_{n=0}^{\infty}\frac{(-1)^n}{(2n+1)n!}[(u_j)^{n+\frac{1}{2}} - (u_{j-1})^{n+\frac{1}{2}}]\}$$

$$\times\{(\frac{4}{\Delta t_j} - \frac{8t_{j-1}}{(\Delta t_j)^2})(\frac{t_s}{2} - \frac{X^2}{4\alpha})$$

$$-\frac{2t_{j-1}}{\Delta t_j} + \frac{2t_{j-1}^2}{(\Delta t_j)^2} - \frac{2t_s^2}{(\Delta t_j)^2}$$

$$+\frac{2t_s X^2}{\alpha\Delta t_j^2} - \frac{X^2}{6\alpha^2(\Delta t_j)^2}\}$$

$$+\frac{X^4}{12\sqrt{\pi}\alpha^2(\Delta t_j)^2}\{\sum_{n=0}^{\infty}\frac{(-1)^n}{n!}[(u_j)^{n-\frac{3}{2}} - (u_{j-1})^{n-\frac{3}{2}}]\}$$

$$+\{\frac{2t_s^2 X^2}{\alpha\sqrt{\pi}(\Delta t_j)^2}$$

$$-\frac{2X^4}{\alpha^2\sqrt{\pi}(\Delta t_j)^2} - \frac{X^2}{\alpha\sqrt{\pi}}(\frac{1}{\Delta t_j} + \frac{2t_{j-1}}{(\Delta t_j)^2})\}$$

$$\times\{\sum_{n=0}^{\infty}\frac{(-1)^n}{n!}[(u_j)^{n-\frac{1}{2}} - (u_{j-1})^{n-\frac{1}{2}}]\}$$

where $u_j = \frac{X^2}{4\alpha(t_s - t_j)}$, $u_{j-1} = \frac{X^2}{4\alpha(t_s - t_{j-1})}$

and $X = X(t_s)$

$$I_{43} = \{\frac{t_{j-1}}{2\Delta t_j} + \frac{t_{j-1}^2}{(\Delta t_j)^2} - (\frac{1}{\Delta t_j} + \frac{4t_{j-1}}{(\Delta t_j)^2})$$

$$\times(\frac{t_s}{2\alpha} - \frac{X^2}{4\alpha}) + \frac{t_s^2}{(\Delta t_j)^2} + \frac{X^4}{12\alpha^2(\Delta t_j)^2} - \frac{t_s X^2}{2\alpha(\Delta t_j)^2}\}$$

$$\times\{\frac{2}{\sqrt{\pi}}\sum_{n=0}^{\infty}\frac{(-1)^n}{(2n+1)n!}[(u_j)^{n+\frac{1}{2}} - (u_{j-1})^{n+\frac{1}{2}}]\} +$$

$$\{\frac{X^4}{12\alpha^2\sqrt{\pi}(\Delta t_j)^2} - \frac{t_s X^2}{\alpha(\Delta t_j)^2}$$

$$-\frac{X^2}{4\alpha\sqrt{\pi}}(\frac{1}{\Delta t_j} + \frac{4t_{j-1}}{(\Delta t_j)^2})\}$$

$$\times\{\sum_{n=0}^{\infty}\frac{(-1)^n}{n!}[(u_j)^{n-\frac{1}{2}} - (u_{j-1})^{n-\frac{1}{2}}]\}$$

$$-\frac{X^4}{24\alpha^2\sqrt{\pi}(\Delta t_j)^2}\times\{\sum_{n=0}^{\infty}\frac{(-1)^n}{n!}[(u_j)^{n-\frac{3}{2}} - (u_{j-1})^{n-\frac{3}{2}}]\}$$

where $u_j = \frac{X^2}{4\alpha(t_s - t_j)}$, $u_{j-1} = \frac{X^2}{4\alpha(t_s - t_{j-1})}$

and $X = X(t_s)$

$$I_{51} = \{(\frac{\alpha t_s}{V} - \frac{2\alpha^2}{V^3})(\frac{3}{\Delta t_j} - \frac{4t_{j-1}}{(\Delta t_j)^2})$$

$$-\frac{\alpha}{V}(1 + \frac{3t_{j-1}}{\Delta t_j} + \frac{2t_{j-1}^2}{(\Delta t_j)^2}) + \frac{2\alpha}{(\Delta t_j)^2}(\frac{4\alpha t_s}{V^3} - \frac{t_s^2}{V} - \frac{12\alpha^2}{V^5})\}$$

$$\times\{\frac{2}{\sqrt{\pi}}\sum_{n=0}^{\infty}\frac{(-1)^n}{(2n+1)n!}[(u_j)^{n+\frac{1}{2}} - (u_{j-1})^{n+\frac{1}{2}}]\}$$

$$+\frac{32\alpha^3}{(\Delta t_j)^2 V^5\sqrt{\pi}}\{\sum_{n=0}^{\infty}\frac{(-1)^n}{n!}[(u_j)^{n+\frac{3}{2}} - (u_{j-1})^{n+\frac{3}{2}}]\}$$

$$+\{\frac{4\alpha^2}{V^3\sqrt{\pi}}(\frac{3}{\Delta t_j}-\frac{4t_{j-1}}{(\Delta t_j)^2})$$

$$+\frac{2\alpha}{(\Delta t_j)^2\sqrt{\pi}}(\frac{24\alpha^2}{V^5}-\frac{6\alpha t_s}{V^3})\}$$

$$\{\sum_{n=0}^{\infty}\frac{(-1)^n}{n!}[(u_j)^{n+\frac{1}{2}}-(u_{j-1})^{n+\frac{1}{2}}]\}$$

where $u_j=\frac{(t_s-t_j)V^2}{4\alpha}$, $u_{j-1}=\frac{(t_s-t_{j-1})V^2}{4\alpha}$,

$V=V(\bar{t}_j)$, $\bar{t}_j=\frac{t_j+t_{j-1}}{2}$

$$I_{52}=\{(\frac{8\alpha^2}{V^3}-\frac{4\alpha t_s}{V})(\frac{1}{\Delta t_j}+\frac{2t_{j-1}}{(\Delta t_j)^2})$$

$$+\frac{4\alpha}{V}(\frac{t_{j-1}}{\Delta t_j}+\frac{t_{j-1}^2}{(\Delta t_j)^2})-\frac{4\alpha}{(\Delta t_j)^2}(\frac{4\alpha t_s}{V^3}-\frac{t_s^2}{V}-\frac{12\alpha^2}{V^5})\}$$

$$\times\{\frac{2}{\sqrt{\pi}}\sum_{n=0}^{\infty}\frac{(-1)^n}{(2n+1)n!}[(u_j)^{n+\frac{1}{2}}-(u_{j-1})^{n+\frac{1}{2}}]\}$$

$$-\frac{64\alpha^3}{(\Delta t_j)^2V^5\sqrt{\pi}}\{\sum_{n=0}^{\infty}\frac{(-1)^n}{n!}[(u_j)^{n+\frac{3}{2}}-(u_{j-1})^{n+\frac{3}{2}}]\}$$

$$-\{\frac{16\alpha^2}{V^3\sqrt{\pi}}(\frac{1}{\Delta t_j}+\frac{2t_{j-1}}{(\Delta t_j)^2})+\frac{4\alpha}{(\Delta t_j)^2\sqrt{\pi}}(\frac{24\alpha^2}{V^5}-\frac{6\alpha t_s}{V^3})\}$$

$$\{\sum_{n=0}^{\infty}\frac{(-1)^n}{n!}[(u_j)^{n+\frac{1}{2}}-(u_{j-1})^{n+\frac{1}{2}}]\}$$

where $u_j=\frac{(t_s-t_j)V^2}{4\alpha}$, $u_{j-1}=\frac{(t_s-t_{j-1})V^2}{4\alpha}$,

$V=V(\bar{t}_j)$, $\bar{t}_j=\frac{t_j+t_{j-1}}{2}$

$$I_{53}=\{(\frac{\alpha t_s}{V}-\frac{2\alpha^2}{V^3})(\frac{1}{\Delta t_j}+\frac{2t_{j-1}}{(\Delta t_j)^2})$$

$$-\frac{\alpha}{V}(\frac{t_{j-1}^2}{(\Delta t_j)^2}+\frac{t_{j-1}}{\Delta t_j})+\frac{2\alpha}{(\Delta t_j)^2}(\frac{4\alpha t_s}{V^3}-\frac{t_s^2}{V}-\frac{12\alpha^2}{V^5})\}$$

$$\times\{\frac{2}{\sqrt{\pi}}\sum_{n=0}^{\infty}\frac{(-1)^n}{(2n+1)n!}[(u_j)^{n+\frac{1}{2}}-(u_{j-1})^{n+\frac{1}{2}}]\}$$

$$-\frac{64\alpha^3}{(\Delta t_j)^2V^5\sqrt{\pi}}\{\sum_{n=0}^{\infty}\frac{(-1)^n}{n!}[(u_j)^{n+\frac{3}{2}}-(u_{j-1})^{n+\frac{3}{2}}]\}$$

$$+\{\frac{4\alpha^2}{V^3\sqrt{\pi}}(\frac{1}{\Delta t_j}+\frac{4t_{j-1}}{(\Delta t_j)^2})+\frac{2\alpha}{(\Delta t_j)^2\sqrt{\pi}}(\frac{24\alpha^2}{V^5}-\frac{6\alpha t_s}{V^3})\}$$

$$\{\sum_{n=0}^{\infty}\frac{(-1)^n}{n!}[(u_j)^{n+\frac{1}{2}}-(u_{j-1})^{n+\frac{1}{2}}]\}$$

where $u_j=\frac{(t_s-t_j)V^2}{4\alpha}$, $u_{j-1}=\frac{(t_s-t_{j-1})V^2}{4\alpha}$,

$V=V(\bar{t}_j)$, $\bar{t}_j=\frac{t_j+t_{j-1}}{2}$

$$I_{61}=\{\frac{3t_s}{2\Delta t_j}+\frac{2t_st_{j-1}}{(\Delta t_j)^2}$$

$$-\frac{1}{2}(1+\frac{3t_{j-1}}{\Delta t_j}+\frac{2t_{j-1}^2}{(\Delta t_j)^2})$$

$$-\frac{\alpha}{V^2}+\frac{4\alpha t_s}{(\Delta t_j)^2V^2}-\frac{t_s^2}{(\Delta t_j)^2}-\frac{12\alpha^2}{(\Delta t_j)^2V^4}\}$$

$$\times\{\frac{2}{\sqrt{\pi}}\sum_{n=0}^{\infty}\frac{(-1)^n}{(2n+1)n!}[(u_j)^{n+\frac{1}{2}}-(u_{j-1})^{n+\frac{1}{2}}]\}$$

$$+\frac{8\alpha}{V^4\sqrt{\pi}}\{\sum_{n=0}^{\infty}\frac{(-1)^n}{n!}[(u_j)^{n+\frac{3}{2}}-(u_{j-1})^{n+\frac{3}{2}}]\}$$

$$+\{\frac{2\alpha}{V^2\sqrt{\pi}}(\frac{3}{\Delta t_j}+\frac{4t_{j-1}}{(\Delta t_j)^2})$$

$$+\frac{4\alpha}{V^4\sqrt{\pi}}(3\alpha-1)\}$$

$$\times\{\sum_{n=0}^{\infty}\frac{(-1)^n}{n!}[(u_j)^{n+\frac{1}{2}}-(u_{j-1})^{n+\frac{1}{2}}]\}$$

where $u_j=\frac{(t_s-t_j)V^2}{4\alpha}$, $u_{j-1}=\frac{(t_s-t_{j-1})V^2}{4\alpha}$,

$V=V(\bar{t}_j)$, $\bar{t}_j=\frac{t_j+t_{j-1}}{2}$

$$I_{62}=\{2[\frac{t_{j-1}}{\Delta t_j}+(\frac{t_{j-1}}{\Delta t_j})^2]-\frac{4t_s t_{j-1}}{(\Delta t_j)^2}$$
$$-\frac{2t_s}{\Delta t_j}+\frac{8\alpha t_{j-1}}{(\Delta t_j)^2V^2}+\frac{4\alpha}{\Delta t_j}$$
$$-\frac{4\alpha}{(\Delta t_j)^2}(\frac{2t_s}{V^2}-\frac{t_s^2}{2\alpha}-\frac{6\alpha}{V^4})\}$$
$$\times\{\frac{2}{\sqrt{\pi}}\sum_{n=0}^{\infty}\frac{(-1)^n}{(2n+1)n!}[(u_j)^{n+\frac{1}{2}}-(u_{j-1})^{n+\frac{1}{2}}]\}$$
$$-\frac{32\alpha^2}{(\Delta t_j)^2V^4\sqrt{\pi}}$$
$$\{\sum_{n=0}^{\infty}\frac{(-1)^n}{n!}[(u_j)^{n+\frac{3}{2}}-(u_{j-1})^{n+\frac{3}{2}}]\}$$
$$-\{\frac{8\alpha}{(\Delta t_j)^2V^4\sqrt{\pi}}(6-2t_s+2t_{j-1}V^2+\Delta t_jV^2)\}$$
$$\{\sum_{n=0}^{\infty}\frac{(-1)^n}{n!}[(u_j)^{n+\frac{1}{2}}-(u_{j-1})^{n+\frac{1}{2}}]\}$$

where $u_j=\frac{(t_s-t_j)V^2}{4\alpha}$, $u_{j-1}=\frac{(t_s-t_{j-1})V^2}{4\alpha}$,

$V=V(\bar{t}_j)$, $\bar{t}_j=\frac{t_j+t_{j-1}}{2}$

$$I_{63}=\{\frac{2\alpha}{(\Delta t_j)^2}(\frac{2t_s}{V^2}-\frac{t_s^2}{2\alpha}-\frac{6\alpha}{V^4})$$
$$+\frac{2t_s t_{j-1}}{(\Delta t_j)^2}+\frac{t_s}{2\Delta t_j}-\frac{1}{2}$$
$$-\frac{\alpha}{V^2}(\frac{4t_{j-1}}{(\Delta t_j)^2}+\frac{1}{\Delta t_j})\}$$
$$\times\{\frac{2}{\sqrt{\pi}}\sum_{n=0}^{\infty}\frac{(-1)^n}{(2n+1)n!}[(u_j)^{n+\frac{1}{2}}-(u_{j-1})^{n+\frac{1}{2}}]\}$$
$$+\frac{16\alpha^2}{(\Delta t_j)^2V^4\sqrt{\pi}}\{\sum_{n=0}^{\infty}\frac{(-1)^n}{n!}[(u_j)^{n+\frac{3}{2}}-(u_{j-1})^{n+\frac{3}{2}}]\}$$
$$+\{\frac{2\alpha}{(\Delta t_j)^2V^4\sqrt{\pi}}(12\alpha-4t_s+4t_{j-1}V^2+\Delta t_jV^2)$$
$$\times\{\sum_{n=0}^{\infty}\frac{(-1)^n}{n!}[(u_j)^{n+\frac{1}{2}}-(u_{j-1})^{n+\frac{1}{2}}]\}$$

where $u_j=\frac{(t_s-t_j)V^2}{4\alpha}$, $u_{j-1}=\frac{(t_s-t_{j-1})V^2}{4\alpha}$,

$V=V(\bar{t}_j)$, $\bar{t}_j=\frac{t_j+t_{j-1}}{2}$

8. REFERENCES

1. Carslaw, H. S. and Jaeger, J. C., "Conduction of Heat in Solids", Oxford University Press, London, (1959).
2. Ozisik, M. N., "Heat Conduction", 2nd. Edition, Wiley and Sons, New York, (1993).
3. Kozdoba, L. A, "Methods of Solving Nonlinear Heat Conduction Problems", Nauka, Moscow, (1975) [in Russian].
4. Bankoff, S. G., "Heat Conduction or Diffusion with Phase Change", In Advances in Chemical Engineering, Academic Press, (1964).
5. Rubinstein, L. I., "The Stefan Problem", Translations From Mathematical Monographs, American Mathematical Society, Rhode Island, Vol. 27, (1971).
6. Ockendon, J. R. and Hodgkins, W. R., "Moving Boundary Problems in Heat Flow and Diffusion", Oxford University Press, Clarendon, London, (1975).
7. Wilson, D. G., Solomon, A. D. and Boggs, P. T., "Moving Boundary Problems", Academic Press, New York, (1978).
8. Crank, J., "Free and Moving Boundary Problems", Clarendon Press, Oxford, (1984).
9. Minkowycz, W. J. et al., "Handbook of Numerical Heat Transfer", Wiley and Sons, New York, (1988).
10. Salcudean, M. and Abdullah, Z., "On the Numerical Modelling of Heat Transfer During Solidification Processes", ***Int. J. Num. Meth. Engng.***, Vol. 25, No. 2, (1988), 445-473.
11. Gradshteyn, I. S. and Ryzhnik, I. M., "Tables of Integrals", Series and Products, 4Th Ed. Academic Press Inc., London, (1965).
12. Tyn Myint U, Debnath, L., "Partial Differential Equations for Scientists and Engineers", 3rd Edition, Elsevier, North-Holland, (1987).
13. Weinberger, H., "A First Course in Partial Differential Equation", Blaisdell, Waltham, Massachusetts, (1965).
14. Solomon, A. D., Wilson, D. G. and Alexiades, A., "The Quasi-Stationary Approximation for the Stefan Problem with Convective Boundary Conditions", ***Int. J. of Mathematics and Mathematical Sciences***, 7, (1984), 549-563.
15. Alexiades, A., "Void Formation in Solidification", in Differential Equations Edited by Dafermos, C.M. and et al., Lecture Notes in Pure and Applied Mathematics, (1989a).
16. Wilson, D. G. and Solomon, A. D., "A Stefan-Type

Problem with Void Formation and Its Explicit Solution", ***IMA J of Applied Mathematics***, 37, (1986), 67-76.
17. Banerjee, P. K., "Boundary Element Method in Engineering", 2nd Edition, McGraw Hill Book Co., (1994).
18. Banerjee, P. K. and Shaw, R. P., "Boundary Element Formulation for Melting and Solidification Problems", Developments in Boundary Element Methods-2 (Banners, P.K. and Shaw, RP eds.), Barking, Essex, UK, (1982), 1-18.
19. O'Neill, K., "Boundary Integral Equation Solution for Moving Boundary Phase Change Problems", ***International Journal for Numerical Methods in Engineering***, 19, (1983), 1825-1850.
20. Heinlein, M et al., "A Boundary Element Method Analysis of Temperature Fields and Stresses During Solidification", ***Acta Mechanica***, 59, (1986), 59-81.
21. Morse, P.M. and Feshbach, H., Methods of Theoretical Physics, McGraw Hill Book Co., New York, (1953).
22. Khoshravan, E., Talati, F., "Numerical Simulation of Solidification Problems by the Boundary Element Method", ***Int'l Conference of Energy, Research and Development (ICERD 2)***, (8-10 April 2002), Kuwait, 256-270